RADIOCARBON, Vol 43, Nr 1, 2001, p 87–118

LEAST-SQUARES FITTING SMOOTH CURVES TO DECADAL RADIOCARBON CALIBRATION DATA FROM AD 1145 TO AD 1945

F B Knox[1] • B G McFadgen[2]

ABSTRACT. Smoothed curves are least-squares fitted to three sets of decadal radiocarbon calibration data from New Zealand and British Isles (AD 1725–1935) and western North America (AD 1145–1945). The curves are compared with each other and with a curve previously calculated from New Zealand data (AD 1335–1745). The smoothing procedure results in reduced standard deviations of the curves, but at the expense of time resolution. The comparison shows a variable ^{14}C offset between the northern and southern hemispheres of 0–70 years (Southern Hemisphere older), and a Northern Hemisphere longitudinal variation of –20 to +60 years (British Isles generally older than western North America).

INTRODUCTION

In a previous paper (McFadgen et al. 1994) it was shown that a simple conversion of radiocarbon dates to calendar dates, using ^{14}C calibration data, results in artificial spreading and clumping of the calendar dates. The effect arises from an interaction between the spread of ^{14}C data due to measurement statistics and changes of slope in the calibration curve, whose effect can be mitigated by reducing the slope changes. While some of the change in calibration curve slope is irreducibly set by geophysical factors, an appreciable fraction on the short time-scale is produced by statistical fluctuations from one calibration point to the next, and can be reduced by the application of appropriate filters.

Subsequently (Knox and McFadgen 1997), a method was presented for achieving a reduction in short time-scale slope changes in the curve by least-squares fitting a Wiener filtered Fourier sum to the data: illustrated on a short ^{14}C-dated Matai tree-ring decadal calibration sequence from New Zealand (Sparks et al. 1995). The present paper applies the method, slightly modified, to the above calibration sequence, and to three other independently measured sets of decadal calibration data. These are the Southern Hemisphere Cedar and Northern Hemisphere Oak data (AD 1725–1935) of McCormac et al. (1998), and a segment (AD 1145–1945) of the Northern Hemisphere Douglas Fir data of Stuiver et al. (1998).

The Douglas Fir data are from a decadal set that is a component of the INTCAL98 ^{14}C age curve (Stuiver et al. 1998). Our method of fitting a smooth curve in no way replaces the careful assessment of errors that has gone into producing the decadal points of the INTCAL98 curve, but is an improvement over simply joining successive decadal points by straight lines to form that curve. Such joining by straight lines, a traditional aid to the eye, is clearly artificial, and does nothing to smooth away the known statistical fluctuations of measurement between nearby decadal points. By contrast, fitting a Wiener filtered Fourier series to the data optimally removes some of this statistical fluctuation at the expense of time resolution. It produces a smooth curve that is optimal in that it is as close as possible (in the least-squares sense) to the true calibration curve (Press et al. 1994: §13.3).

The Douglas Fir curve calculation is here limited to using data later than AD 1140 as the segment just prior to this includes some irregularly spaced data, the correct processing of which requires modification of our method.

[1]900 Ohariu Valley Road, R.D., Johnsonville, Wellington, New Zealand. Email: fbmoknox@actrix.gen.nz.
[2]Conservation Sciences Centre, Department of Conservation, P.O.Box 10420, Wellington, New Zealand.
Email: bmcfadgen@doc.govt.nz, mcfadgen@actrix.gen.nz.

https://doi.org/10.1017/S0033822200031672 Published online by Cambridge University Press

In addition to their direct use in calibration, the smoothed curves should facilitate comparison of the Northern and Southern Hemisphere data, to find how closely ^{14}C variation matches in the two hemispheres. Such comparison can shed light on the relevant geophysical processes that produce the wiggles in the calibration curves.

METHOD

Detrending

The procedure for least-squares fitting Fourier sums to the data points follows that given by Knox and McFadgen (1997) for Sparks et al.'s (1995) Matai data, except for detrending. Detrending in the above paper was achieved simply by subtracting points on the ideal straight line representing ^{14}C versus tree-ring age (AD 1950 equivalent to BP 0) from corresponding data points. The procedure works well in the earlier case as the endpoint data values differ from the ideal by no more than one or two years, but this happy coincidence does not hold for data segments in general. Detrending in this paper is achieved by the slightly more complicated procedure of subtracting from the data corresponding points on a straight line joining the endpoints of the data segment. As before, the trend is eventually restored to give the final answer.

Any straight line detrending procedure on a finite set of discrete data will introduce spurious high-frequency components to the data set, not all of which are cancelled when the trend is restored. This comes about through the phenomenon called aliasing (Press et al. 1994:§12.1). The non-cancellable frequencies lie above the Nyquist frequency (the inverse of twice the sampling period), whose frequency, for decadal sampling is 0.05 yr^{-1} (Figure 1). It can be shown that detrending by subtracting the straight line joining the endpoints of the data segment introduces less power at frequencies that can be aliased than the alternative of detrending by subtracting the best fit straight line, with its generally discontinuous jumps to zero at the ends of the data segment. Detrending by subtracting the straight line joining the endpoints only introduces a corresponding discontinuity of slope.

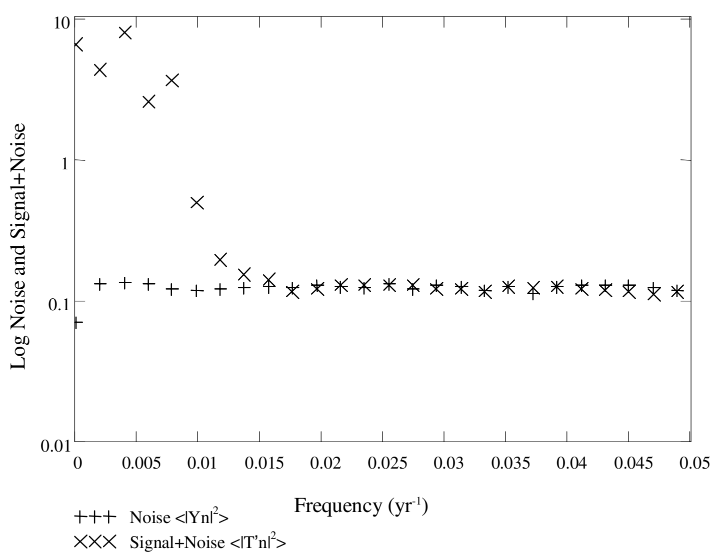

Figure 1 Spectrum of noise power compared with signal+noise power for Matai calibration curve data.

https://doi.org/10.1017/S0033822200031672 Published online by Cambridge University Press

Aliasing errors in a curve detrended by subtracting the straight line joining data end-points is then less (in our case by one to two orders of magnitude) than for a curve detrended by subtracting the best-fit straight line. This explains the small differences, concentrated near the ends, between the differently detrended Matai curves illustrated in Figure 2.

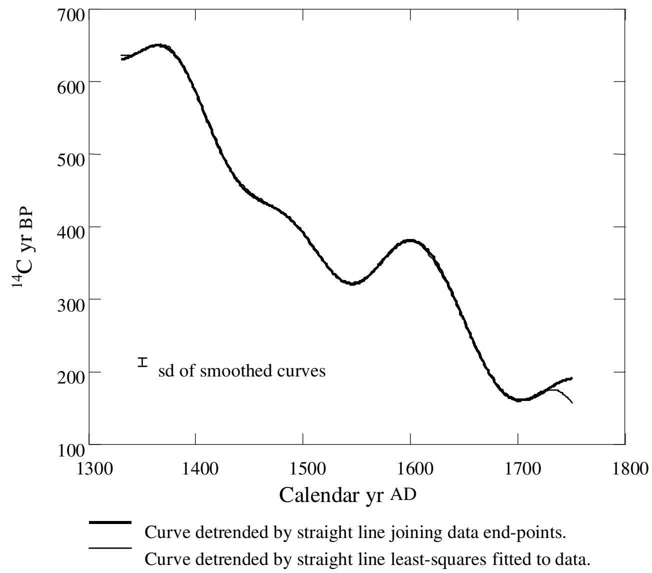

Figure 2 Comparison of Matai calibration curves detrended by the straight line joining data end-points, and detrended by the straight line least-squares fitted to the data points. χ^2 statistic for curve detrended by straight line joining data end-points = 9.98, and for curve detrended by least-squares fitted straight line to the data points = 8.27. ($\chi^2_{0.95}$ = 11.07, d.f. =5). Note the slight divergence of the two curves at each end of the plot. Standard deviation of the smoothed curves shown as sd.

Since the aliasing errors in the curve detrended by subtracting the straight line joining the data end-points are one to two orders of magnitude smaller than in the curve detrended by subtracting the least-squares fitted line, most of the difference between the ends of the two curves in Figure 2, a difference of up to 30 years, is expected to be due to aliasing in the least-squares detrended curve. This implies error at the ends of the curve detrended by subtracting the straight line joining data end-points is one to two orders of magnitude smaller than 30 years, say not more than 3 years at the outside and small compared with the 9 years estimated for the standard deviation of the Matai calibration curve. This 3-year upper limit to the error generated by aliasing is also small compared with the standard deviations of the other calibration curves, except the AD 1515–1945 Douglas Fir curve. In the last case the 3-year upper limit equals the standard deviation but would be covered by increasing to 4 years the standard deviation at the curve ends.

In situations where there are many thousands or more of data points, the power in the aliased frequencies is proportionately small enough not to matter in either method of detrending, and it is usual to subtract the best-fit straight line. However, here the small number of data points (22–44) allows a detectable error to creep in when detrending is by the least-squares straight line. Although both Matai curves pass the statistical Chi-squared test (see later), in light of the above discussion on aliasing, we have opted for detrending by subtracting the straight line joining data end-points.

Filtering

The procedure for least-squares fitting Fourier sums to the data involves obtaining the Fourier transform of the chosen section of detrended data, filtering out as much as possible of the statistical fluctuations in the data set, and then inverse Fourier transforming the result to get a least-squares fitted smooth curve to the detrended data. Finally, the trend is added back to give the corresponding curve through the original calibration data.

Along with filtering the statistical fluctuations, opportunity is taken to apply an extra filter to compensate somewhat for the decadal averaging inherent in the data points: R_n in equation (8).

The filter used for removing the statistical fluctuations is the optimal Wiener filter, which, in the notation of Press et al. (1994: §13.3), weights a Fourier component of frequency f by multiplying by $\Phi(f) = |S(f)|^2/(|S(f)|^2 + |N(f)|^2)$, where $|S(f)|^2$ is the power spectrum of the desired signal, and $|N(f)|^2$ is the power spectrum of the statistical fluctuations or noise (Press et al. 1994).

Since the power spectrum of the signal and noise together, say $|C(f)|^2$, is what is actually measured, and is approximately equal to $|S(f)|^2 + |N(f)|^2$ (Press et al. 1994), we can put $\Phi(f) = 1 - |N(f)|^2/|C(f)|^2$, which, in the notation of our earlier paper (Knox and McFadgen 1997: equation [9]), is

$$\langle \Phi'_n \rangle = 1 - \langle |Y_n|^2 \rangle / \langle |T'_n|^2 \rangle \tag{1}$$

In order to calculate $\langle |Y_n|^2 \rangle$ we take the statistical fluctuations in the decadal data points as being distributed normally about zero with the standard deviations given, and calculate a discrete Fourier transform

$$Y_n = \sum_{k=0}^{N-1} \nu_k e^{2\pi ikn/N} \tag{2}$$

(Knox and McFadgen 1997, equation [5]), where a value ν_k is obtained as a number of years selected randomly from a normal distribution (mean zero) with standard deviation equal to that given for the kth data point. All values of ν_k in the range $0 \le k \le N-1$ other than those corresponding to the data points are put equal to zero, the same procedure as for obtaining the Fourier transform of the calibration data set itself (Knox and McFadgen 1997, equation [1]). The power spectrum of Y_n is now $|Y_n|^2$ the square of the modulus of Y_n, a discrete function of the frequency f = n/N in units of reciprocal years (yr^{-1}).

In any independent run of the Y_n power spectrum only one randomly chosen value of ν_k is used at each value of k. Different runs of randomly chosen values were generally found to give very irregular spectra, varying appreciably from one run to the next. However, an average of 500 independent runs produces an acceptably constant and smooth spectrum, denoted here by $\langle |Y_n|^2 \rangle$.

The same problem occurs in calculating $\langle |T_n|^2 \rangle$, because each τ_k (see below) is measured only once, and only one set of data is available; but overcoming the problem requires a more elaborate procedure than that given for calculating $\langle |Y_n|^2 \rangle$: we first calculate the discrete Fourier transform of the noisy calibration data

$$T_n = \sum_{k=0}^{N-1} \tau_k e^{-2\pi ikn/N} \tag{3}$$

https://doi.org/10.1017/S0033822200031672 Published online by Cambridge University Press

(Knox and McFadgen 1997, equation [1]), where τ_k are the detrended ^{14}C calibration data values in years, listed in Table 1 of the present paper (see Appendix). As in the case of Y_n, the power spectrum of the noisy data is now $|T_n|^2$ (the square of the modulus of T_n), and a preliminary filter

$$\Phi'_n = 1 - \langle |Y_n|^2 \rangle / |T_n|^2 \tag{4}$$

Knox and McFadgen 1997, equation [6]) is used to make a first estimate of the detrended calibration curve, by inverse Fourier transforming the product $\Phi'_n T_n$ (Knox and McFadgen 1997, equation [7]):

$$\theta'_k = \frac{D}{N} \sum_{n=0}^{N-1} \Phi'_n T_n e^{-2\pi ikn/N} \tag{5}$$

where D (the spacing in years between decadal points) is a normalizing factor (Knox and McFadgen 1997:197). Now, as in the case of Y_n, we calculate a Fourier transform

$$T'_n = \sum_{k=0}^{N-1} \tau'_k e^{2\pi ikn/N} \tag{6}$$

where a set of τ'_k is obtained by taking the set of k values of the above first estimate of the detrended calibration curve, θ'_k, and adding to them a particular set of the ν_k calculated previously, i.e.

$$\tau'_k = \theta'_k + \nu_k \tag{7}$$

This is repeated for all 500 independent sets of ν_k, and the corresponding 500 independent estimates of $|T'_n|^2$ averaged to give the $\langle |T'_n|^2 \rangle$ used to calculate $\langle \Phi'_n \rangle$ in equation (1).

Since the ν_k are distributed normally about zero, the τ'_k are distributed normally about θ'_k, making a spectrum which is the sum of both signal and noise power, distinct from $|Y_n|^2$ the power spectrum of noise only.

Sufficiently large averages of $|T'_n|^2$ and $|Y_n|^2$ converge to the two distinct power spectra $\langle |T'_n|^2 \rangle$ and $\langle |Y_n|^2 \rangle$ plotted against frequency (n/N) in Figure 1. Even averaged over 500 simulations there is still appreciable statistical fluctuation in the spectra, obvious in the high frequency region where at some frequencies the difference between signal plus noise and noise alone is negative. Since this difference must be positive, where it is negative the signal must be negligible compared with the noise. Accordingly we take the signal to be negligible compared with noise for all cases where the difference between signal plus noise and noise alone (regardless of sign) is less than or equal to the largest magnitude of the observed negative difference. In Figure 1 this occurs for all frequencies above 0.01367 yr^{-1}, and the corresponding part of the Wiener filter is set equal to zero. Also, since the statistical fluctuations in the long run average to zero, ideally the zero frequency component of the noise is zero, i.e. $|N(0)|^2 = 0$ and $\Phi(0) = 1$. The complete Wiener filters, together with signal to noise values, are given in Table 2.

Now, points on the detrended calibration curve are given by

$$\theta_k = \frac{D}{N} \sum_{n=0}^{N-1} \frac{\langle \Phi'_n \rangle}{R_n} T_n e^{-2\pi ikn/N} \tag{8}$$

https://doi.org/10.1017/S0033822200031672 Published online by Cambridge University Press

Table 2 Wiener filters (= $\langle \Phi'_n \rangle$) and ratios of signal/noise (=($|S|^2/|N|^2$) for smoothed calibration curves. Note: weighting of the terms in the Fourier sum = $\langle \Phi'_n \rangle$ T_n/R_n (see Equation 8).

	Matai AD 1335–1745		Douglas Fir AD 1145–505		Douglas Fir AD 1515–1945		Oak AD 1725–1935		Cedar AD 1725–1935	
Frequency (y^{-1})	$\langle \Phi'_n \rangle$	$\|S\|^2/\|N\|^2$	$\langle \Phi'_n \rangle$	$\|S\|^2/\|N\|^2$	$\langle \Phi'_n \rangle$	$\|S\|^2/\|N\|^2$	$\langle \Phi'_n \rangle$	$\|S\|^2/\|N\|^2$	$\langle \Phi'_n \rangle$	$\|S\|^2/\|N\|^2$
0	1.000	∞	1.000	∞	1.000	∞	1.000	∞	1.000	∞
0.001953125	0.969	31	0.895	8.5	1.000	∞	0.982	55	0.983	58
0.003906250	0.983	58	0.886	7.8	0.997	330	0.988	82	0.986	70
0.005859375	0.948	18	0.985	66	1.000	∞	0.976	41	0.968	30
0.007812500	0.966	28	0.985	66	0.995	200	0.926	13	0.913	10
0.009765625	0.758	3.1	0.926	13	0.978	44	0.938	15	0.942	16
0.011718750	0.369	0.58	0.750	3.0	0.991	110	0.885	7.7	0.901	9.1
0.013671875	0.194	0.24	0.575	1.4	0.990	99	0.438	0.78	0.574	1.3
0.015625000	0	0	0.732	2.7	0.983	58	0.379	0.61	0.672	2.0
0.017578125	0	0	0.871	6.8	0.978	44	0.146	0.17	0.477	0.91
0.019531250	0	0	0.256	0.34	0.894	8.4	0.750	3.0	0.756	3.1
0.021484375	0	0	0.141	0.16	0.980	49	0.794	3.9	0.852	5.8
0.023437500	0	0	0	0	0.873	6.9	0.510	1.0	0.737	2.8
0.025390625	0	0	0	0	0.879	7.3	0	0	0	0
0.027343750	0	0	0	0	0.420	0.72	0	0	0	0
0.029296875	0	0	0	0	0	0	0	0	0	0
0.031250000	0	0	0	0	0	0	0	0	0	0
0.033203125	0	0	0	0	0	0	0	0	0	0
0.035156250	0	0	0	0	0	0	0	0	0	0
0.037109375	0	0	0	0	0	0	0	0	0	0
0.039062500	0	0	0	0	0	0	0	0	0	0
0.041015625	0	0	0	0	0	0	0	0	0	0
0.042968750	0	0	0	0	0	0	0	0	0	0
0.044921875	0	0	0	0	0	0	0	0	0	0
0.046875000	0	0	0	0	0	0	0	0	0	0
0.048828125	0	0	0	0	0	0	0	0	0	0

(Knox and McFadgen 1997, equation [10]), where R_n is a function correcting decadal averaging in the data (Knox and McFadgen 1997, equation [3]). Finally the optimally least-squares fitted curve is produced by adding back the initially removed trend.

Optimally least-squares fitted curves to the Matai data, detrended in the two ways discussed earlier, are plotted for comparison in Figure 2. The Matai curve, detrended by joining its end-points, is given in the Appendix (Table 6), and is not significantly different from the curve in our earlier paper (Knox and McFadgen 1997, appendix).

Strictly speaking the filter $\langle \Phi'_n \rangle$ calculated in equation (1), while optimal for the smooth curve passing through the set of values θ'_k, is not quite optimal for estimating the true curve giving rise to the original set of calibration data. Nevertheless, for this data it will be near optimal to the extent that the curve passing through the θ'_k approximates the true calibration curve; the more so in that, as pointed out by Press et al. (1994), results obtained by optimal filtering differ from the true curve by an amount that is second order in the precision to which the optimal filter is determined.

In fact, Press et al. further point out that a plot of $|C(f)|^2$ versus f will often show the spectral signature of a signal rising above a continuous spectrum which can be inferred to be noise (as can be seen in our Figure 1), and suggest that in this case it is sufficient to just extrapolate by eye the noise spectrum through the signal to obtain the full range of $|N(f)|^2$. However, in our case we are better off, in that we know the structure and magnitude of the noise, and can calculate $|N(f)|^2$ independently of

https://doi.org/10.1017/S0033822200031672 Published online by Cambridge University Press

$|C(f)|^2$. The above indicates optimal Wiener filtering is a robust method for separating signal from noise in the situation considered here.

Next we check how well the true calibration curve has been estimated by applying the standard Chi-squared statistical test for normality (Snedecor and Cochran 1967:84) to the distribution of the original data points about corresponding decadal averages derived from the estimated curve. The Chi-squared check is completely independent of the methods used here to derive the estimated curve. Results of the Chi-squared test are given in Table 3 and Figure 2.

Table 3 Chi-square test statistic, mean standard deviation and standard error of standard deviation of the estimated true calibration curves. $\chi^2_{0.95}$=11.07, d.f.= 5. The chi-square statistic is calculated by taking the observed difference between each data point and the local decadal average of the smoothed curve divided by the standard deviation of the data point, and testing the resulting frequency distribution against that predicted by the normal distribution. Cell expectations at the extremes of the distribution are combined so that their sum is more than 1 (Snedecor and Cochran 1967).

	Matai (AD 1335–1745)	Douglas Fir (AD 1145–1505)	Douglas Fir (AD 1515–1945)	Oak (AD 1725–1935)	Cedar (AD 1725–1935)
Chi-square test statistic	9.98	9.64	4.05	6.56	2.73
Mean sd	9	8	3	8	8
Se of sd	3	3	1	4	3

The likely error in the estimation of a true calibration curve was determined by taking a decadal average of the estimated curve about each calendar date corresponding to an original data point, and adding to it a number of years selected randomly from a normal distribution with standard deviation equal to that of the corresponding data point. These values along with their corresponding calendar dates constitute a simulated data set from which a simulated calibration curve can be recovered by the procedure described in this paper.

For each calibration curve estimated from the real data, 500 simulated curves were constructed, and at any given calendar date of a calibration curve the 500 simulated calibration points were found to be distributed normally with standard deviations not significantly different at the different calendar dates. An average of these standard deviations over the range of calendar dates is given as a measure of error in the corresponding estimation of the true calibration curve.

In our previous paper (Knox and McFadgen 1997) we had not determined that the estimated points of the true calibration curve were distributed normally, and so could only claim the estimated standard deviation to be nominal. Here, and now also in the earlier paper, we can take quoted standard deviations to have their usual strict interpretation.

RESULTS AND COMPARISON OF CURVES

The same processing as for the Matai data was applied to the Douglas Fir, Oak, and Cedar data. The Douglas Fir data falls into two separate parts: a part AD 1145–1505 having consistently higher standard deviations (root-mean-square value 13 yr), and a part AD 1515–1945 having consistently lower standard deviations (root-mean-square value 4 yr), see Table 1. These parts were processed separately.

The standard deviations for the Matai and other estimated curves are given in Table 4, and the Matai calibration curve itself in the Appendix (Table 6) and Figures 2 and 4a. Results of processing the

https://doi.org/10.1017/S0033822200031672 Published online by Cambridge University Press

Douglas Fir, Oak, and Cedar data are given in the Appendix (Tables 7 to 10). The Douglas Fir curve for AD 1140–1510 is plotted in Figure 3, overlaid, for comparison, with the corresponding section of the INTCAL 98 curve. The Matai, Oak and Cedar curves, and both sections of the Douglas Fir curve are plotted and compared in Figures 4a,b.

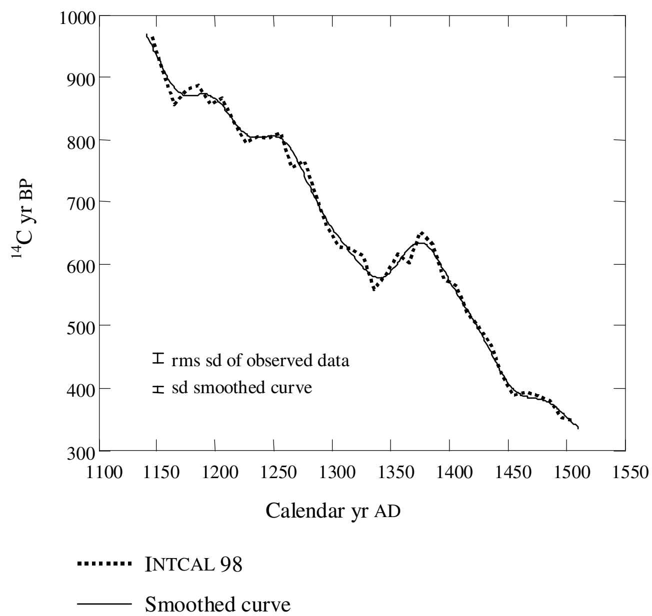

Figure 3 Comparison of the observed Douglas Fir ^{14}C (AD 1145–1505) INTCAL 98 curve and the smoothed curve. Note the reduced standard deviation of the smoothed curve (8yr) compared with the root-mean-square standard deviation of the observed data (13yr).

The standard deviation of a point on the estimated true calibration curve, row 4 of Table 4, is in all cases less than the root-mean-square standard deviation of the raw data, row 2 of Table 4. This is because each point on the estimated calibration curve is effectively a running mean over several data points. The time interval over which the data is effectively averaged is approximately the interval corresponding to the filter frequency at which the ratio of signal to noise power falls below one, and these time intervals are listed in row 1 of Table 4.

Taking the Matai example in Table 4, since the raw data is taken at 10 yr intervals the 45 yr averaging by the Wiener filter reduces the root-mean-square standard deviation of 20 yr to $\sqrt{10/45}$ times 20 yr, i.e. 9 yr. This approximate estimate of the standard deviation of a point on the Matai curve, along with corresponding estimates for the other curves, is given in row 3 of Table 4.

Comparison of rows 3 and 4 of Table 4 shows good agreement between the above approximate estimates of the standard deviations and the standard deviations measured over the sets of 500 simulated calibration curves. Thus the reduction in standard deviation for the calibration curves is obtained at the expense of time resolution, but the lost short term variations in the curve estimates are of amplitude so small as to be obscured in any case by the statistical fluctuations in the raw data.

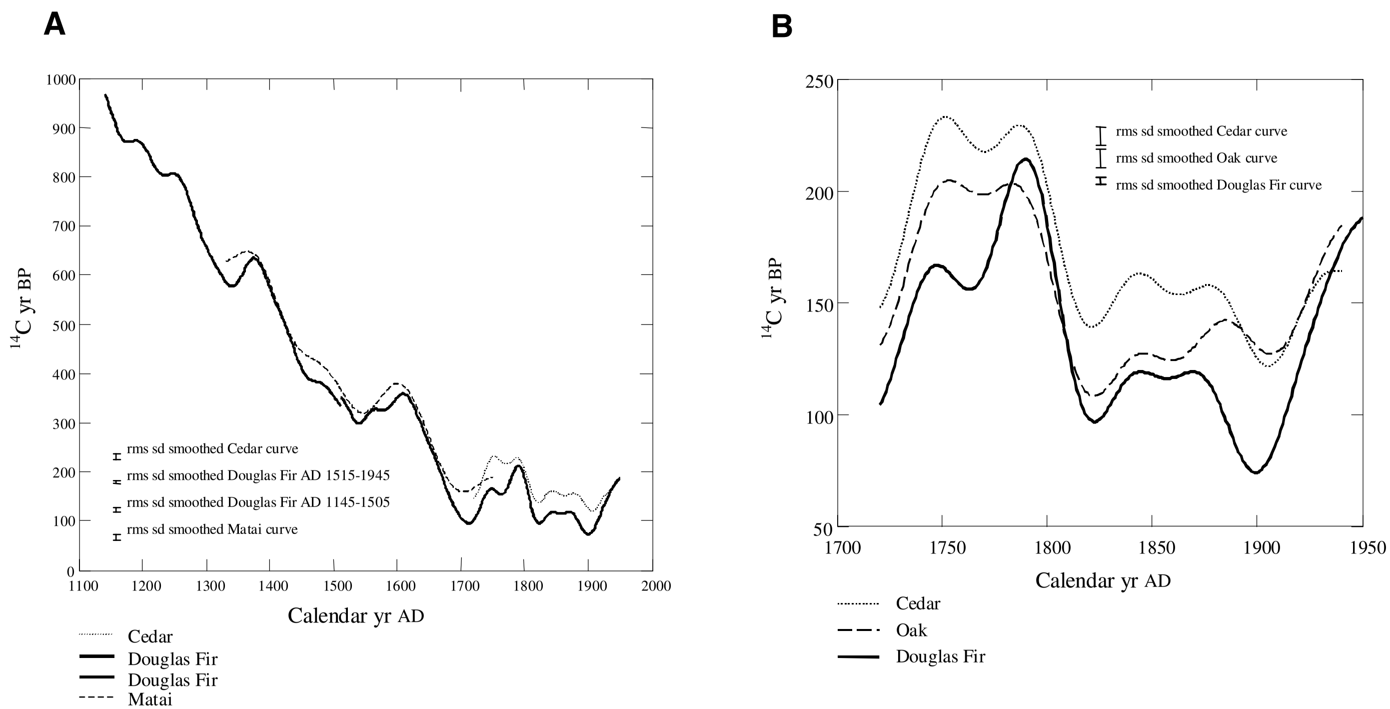

Figure 4 Comparison of smoothed calibration curves for the northern and southern hemispheres. Figure 4a shows Northern Hemisphere curve from AD 1140 to AD 1950 using North American Douglas Fir (*Pseudotsuga menziesii*). Southern Hemisphere curve from AD 1330 to AD 1750 using New Zealand Matai (*Prumnopitys taxifolia*) and from AD 1720 to AD 1940 using New Zealand Cedar (*Libocedrus bidwillii*). Figure 4b shows smoothed calibration curves for Cedar, Oak (*Quercus petroca*), and Douglas Fir from AD 1720 to AD 1950.

Time resolution for the calibration curves can be taken as approximately the values given in row 1 of Table 4.

The presence of shorter time variations in the Douglas Fir, Oak and Cedar curves results in larger corrections for the ten year averaging in the data points of these curves than for the ten year averaging in the Matai data points. By evaluating θ_k with and without the factor R_n (see Equation 8), and comparing the results, it is found that the corrections can be up to three ^{14}C years for the first three curves compared with up to one year for the Matai curve.

Table 4 Comparison of standard deviation of 500 samples of the estimated true calibration curve with approximate standard deviation obtained by averaging the data over an interval long enough to suppress time variation for which $(|S|^2/|N|^2)<1$.

	Matai (AD 1335–1745)	Douglas Fir (AD 1145–1505)	Douglas Fir (AD 1515–1945)	Oak (AD 1725–1935)	Cedar (AD 1725–1935)
Approx. interval over which data effectively averaged (yr)	45	27	18	21	21
Root-mean-square standard deviation of data (yr)	20	13	4	14	13
Expected approx. standard deviation of point on curve (yr)	9	8	3	10	9
Actual standard deviation of point on curve (yr)	9	8	3	8	8

The reason for processing the Douglas Fir data in two separate parts is as follows. As discussed above, the time interval over which data is effectively averaged is the period corresponding to the frequency at which the ratio of signal to noise power is one, and the noise power is determined by the root-mean-square average of the standard deviations of the data set. In those parts of the data set where the standard deviations are systematically and significantly smaller than elsewhere the time interval over which the local data are averaged, set by the average standard deviation over the whole data set, is longer than is locally optimal. In such parts of the data set the estimated calibration curve in general will not follow the data points as closely as it should. Similarly, in those parts of the data set where the standard deviations are larger than elsewhere, requiring but not having an extra long averaging time to smooth away the noise, the calibration curve will follow the data points more closely than it should. Where the above effect is significant the Chi-squared test for a normal distribution of data points about local decadal averages of the curve will not be passed.

The above defect in our method of estimating a calibration curve is overcome by separating the data into sequences with approximately constant root-mean-square running mean averages of the standard deviations.

In the data sets used in this paper the standard deviations averaged over the appropriate number of data points (determined a posteriori using the time resolution intervals in Table 4 above) vary on average by not more than 13%, with extremes not more than 34%, and the corresponding calibration curves pass the appropriate Chi-squared tests. By contrast the two parts of the Douglas Fir data, with their root-mean-square standard deviations differing by a factor of ~3, when processed together as one set of data do not pass the Chi-squared test.

Examination of Figure 4a and the ^{14}C dates at AD 1510 in the Appendix (Tables 7 and 8) shows acceptable agreement between estimates of the true ^{14}C age at AD 1510 in the two abutting Douglas Fir curves. The difference between the two estimates is 16 ± 9 yr, where the standard deviation of 9 yr is taken as the square root of the sum of the variances of the two curves (Table 4).

Figure 4a also shows the Matai curve continuing approximately into the Cedar curve, as would be expected since both trees used grew in the same region of the globe (Table 5). However, closer examination of the overlap of these curves shows the difference between them, though small, to be statistically significant. The difference (Cedar minus Matai) varies from −21 ± 12 to +41 ± 12 yr, where the standard deviation of the differences is the square root of the sum of the variances of the Cedar and Matai curves (Table 4).

Table 5 Global locations of trees used: taken from Stuiver and Becker (1986), McCormac et al. (1998), and R J Sparks (personal communication)

Tree	Latitude	Longitude	Location
Douglas Fir	47°46′N	124°06′W	West coast USA (two trees)
	46°45′N	121°45′W	West coast USA
	43°07′N	123°40′W	West coast USA
	47° N	122° W	West coast USA
	48°40′N	123°40′W	West coast Canada
English Oak	53°12′N	01°04′W	Middle England
	54°44′N	06°16′W	North coast, Ulster
New Zealand Cedar	39°32′S	175°44′E	Middle North Island,
New Zealand Matai	44° S	171° E	Middle east coast, South Island, New Zealand

Since the Cedar and Matai curves are detrended by subtracting lines joining their data end points, aliasing errors, which concentrate at the ends of an estimated curve, should be one to two orders of magnitude less than the maximum of 30 yr shown in Figure 2 for a curve detrended by subtracting a best fit straight line. Part of the difference between points on the estimated Cedar and Matai curves may be due to aliased end errors, but by not more than three years.

On the other hand, a more detailed examination of where the trees grew suggests the difference between the above curves could also be real. The Cedar wood is from a tree that grew in the center of North Island, New Zealand, while the Matai wood is from a tree which grew halfway along the east coast of South Island, New Zealand. North Island is surrounded by subtropical water (Carter et al. 1998), while the east coast of South Island faces the subtropical front, a relatively sharp, fluctuating boundary between subtropical and subantarctic water. If the $^{14}C/^{12}C$ ratio is different in the ventilated carbon dioxide from the subtropical and subantarctic waters we can expect corresponding differences in this ratio in the Cedar and Matai wood, depending on differences in prevailing wind directions at the two sites.

Furthermore, at times the Cedar tree would have been exposed to carbon dioxide vented from North Island's central volcanic plateau, including Mount Ruapehu, an intermittently active volcano some 25 km away, which carbon dioxide may have a reduced $^{14}C/^{12}C$ ratio. However, we cannot say to what extent this effect would be significant. Geochemistry of the tree rings might give some indication.

Coming now to a general comparison of all the calibration curves, Figures 4a,b and 5 show the Matai and Cedar curves to generally give older ^{14}C ages than the Douglas Fir. The average difference in age, up to AD 1900, is seen to support in order of magnitude the recommendation by Stuiver et al.

(1998) to reduce Southern Hemisphere ^{14}C ages by 24 yr prior to calibration. The difference, however, is highly variable: from a maximum of more than 60 yr, which is more than seven standard deviations and highly significant (P<<0.0001), to virtually zero (within one standard deviation). Sparks et al. (1995), Stuiver and Braziunas (1998), and McCormac et al. (1998) also report temporal variation in the interhemispheric offset.

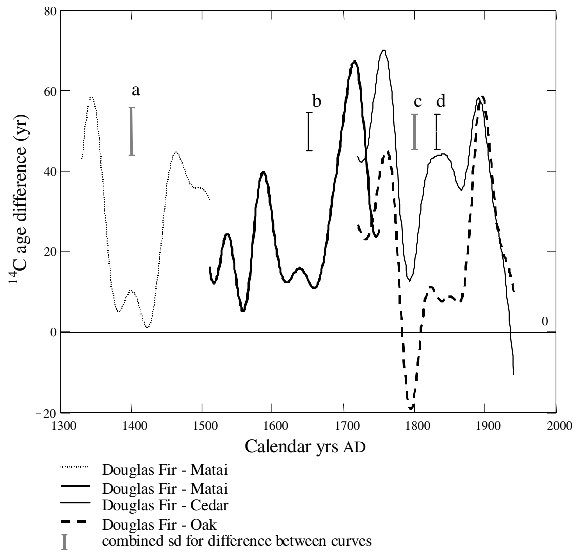

Figure 5 Difference in ^{14}C years between curves for northern and southern hemispheres (Douglas Fir–Matai, Douglas Fir–Cedar), and between western North America and Britain (Douglas Fir–Oak). Combined standard errors for differences between pairs of curves shown by error bars: a=Douglas Fir (AD 1330 to 1510)–Matai, b=Douglas Fir (AD 1510 to 1750)–Matai, c=Douglas Fir (AD 1720 to 1940)–Cedar, d=Douglas Fir (AD 1720 to 1940)–Oak.

An interesting feature of the variability is that, with one exception, the minimum difference occurs at times (~AD 1380–1430, ~AD 1550, ~AD 1610–1660, ~AD 1800: see Figure 5) when the calibration curves are most rapidly descending (Figures 4a,b). The exception (~AD 1930–1940) occurs where the curves are rapidly rising, but, as pointed out by McCormac et al. (1998) and Stuiver et al. (1998), by this time there is appreciable injection of fossil fuel carbon into the atmosphere. Consistent with this view Figure 4b shows all three curves rising to older ^{14}C ages at this time. Thus the exception may not be due entirely to natural causes.

A further interesting feature is that the Northern Hemisphere Oak and Douglas Fir curves do not always agree. There is good agreement between them from AD 1780–1870, but earlier, ~AD 1760, the Oak curve is significantly older by more than five standard deviations (P<<0.0001), and actually closer to the Southern Hemisphere Cedar curve. Later, ~AD 1880–1910, there is no significant difference between the Oak and Cedar curves while both give ^{14}C ages some 60 yr older than the Douglas Fir: almost as large a difference as occurs anywhere in Figures 4 and 5. This difference between Oak and Douglas Fir is more than six standard deviations and highly significant (P<<0.0001). Also the average difference between Oak and Douglas Fir ^{14}C ages up to AD 1900, at 19 +/–3 years, falls little short of the average difference between Southern and Northern Hemisphere ages giving rise to Stuiver et al.'s (1998) recommended 24-year correction.

The significant (though small) differences between the Oak and Douglas Fir curves might be expected: the Oaks grew on the prevailing leeward side of the North Atlantic Ocean whereas the Douglas Firs grew on the prevailing leeward side of the North Pacific. Ventilated carbon dioxide from these different oceans may have different $^{14}C/^{12}C$ ratios.

ACKNOWLEDGMENTS

For the benefit of their discussion we thank Dr Rodger Sparks, Rafter Radiocarbon Laboratory, Institute of Geological and Nuclear Sciences, Gracefield, and Dr Lionel Carter, National Institute of Water and Atmospheric Research, Wellington.

REFERENCES

Carter L, Garlick RD, Sutton P, Chiswell S, Oien NA, Stanton BR. 1998. *Ocean Circulation New Zealand*. NIWA Miscellaneous Chart Series No. 76.

Knox FB, McFadgen BG. 1997. Least-squares fitting a smooth curve to radiocarbon calibration data. *Radiocarbon* 39(2):193–204.

McCormac FG, Hogg AG, Higham TFG, Lynch-Stieglitz J, Broecker WS, Baillie MGL, Palmer J, Pilcher JR, Brown D, Hope ST. 1998. Temporal variation in the interhemispheric ^{14}C offset. *Geophysical Research Letters* 25(9):1321–4.

McFadgen BG, Knox FB, Cole TRL. 1994. Radiocarbon calibration curve variations and their implications for the interpretation of New Zealand prehistory. *Radiocarbon* 36(2):221–36.

Press WH, Teukolsky SA, Vetterling WT, Flannery BP. 1994. *Numerical Recipes in FORTRAN*. 2nd ed. corr. Cambridge: Cambridge Univ. Press. 963 p.

Snedecor G.W, Cochran WG. 1967. *Statistical Methods*. 6th ed. Iowa State University Press. 593 p.

Sparks RJ, Melhuish WH, McKee JWA, Ogden J, Palmer JG, Molloy BPJ. 1995. ^{14}C calibration in the Southern Hemisphere and the date of the last Taupo eruption: Evidence from tree-ring sequences. *Radiocarbon* 37(2):155–63.

Stuiver M, Becker B. 1986. High-precision decadal calibration of the radiocarbon time scale, AD 1950–BC 2500. *Radiocarbon* 28(2B):863–910.

Stuiver M, Braziunas TF. 1998. Anthropogenic and solar components of hemispheric ^{14}C. *Geophysical Research Letters* 25:329–32.

Stuiver M, Reimer PJ, Braziunas TF. 1998. High-precision radiocarbon age calibration for terrestrial and marine samples. *Radiocarbon* 40(3):1127–51

APPENDIX

Table 1 ^{14}C age of tree-ring dated wood of New Zealand Matai (*Prumnopitys taxifolia*) from Sparks et al. (1995: Table 2), Douglas Fir (*Pseudotsuga menziesii*) from Stuiver et al. (1998), and English Oak (*Quercus petroca*), and New Zealand Cedar (*Libocedrus bidwillii*) from McCormac et al. (1998)

Calendar age (AD)	Conventional ^{14}C age (BP)	Standard error (yr)	k[a]	Detrended data τ_k (yr)
Matai AD 1335–1745				
1335	617	22	50	0
1345	635	19	60	–28
1355	639	20	70	–42
1365	683	20	80	–96
1375	637	22	90	–60
1385	618	17	100	–51
1395	593	19	110	–36
1405	599	19	120	–52
1415	530	20	130	7
1425	471	21	140	56
1435	484	21	150	33
1445	422	21	160	85
1455	453	17	170	44
1465	450	19	180	37
1475	420	22	190	57
1485	417	17	200	50
1495	380	23	210	77
1505	380	21	220	67
1515	372	15	230	65
1525	334	21	240	93
1535	323	15	250	94
1545	324	14	260	82
1555	322	18	270	74
1565	307	22	280	79
1575	377	25	290	–1
1585	385	26	300	–19
1595	396	21	310	–40
1605	361	12	320	–15
1615	367	17	330	–31
1625	360	21	340	–34
1635	286	18	350	30
1645	288	20	360	18
1655	290	16	370	6
1665	220	20	380	66
1675	163	22	390	113
1685	163	20	400	103
1695	182	23	410	74
1705	167	21	420	79

https://doi.org/10.1017/S0033822200031672 Published online by Cambridge University Press

Table 1 ^{14}C age of tree-ring dated wood of New Zealand Matai (*Prumnopitys taxifolia*) from Sparks et al. (1995: Table 2), Douglas Fir (*Pseudotsuga menziesii*) from Stuiver et al. (1998), and English Oak (*Quercus petroca*), and New Zealand Cedar (*Libocedrus bidwillii*) from McCormac et al. (1998) (*Continued*)

Calendar age (AD)	Conventional ^{14}C age (BP)	Standard error (yr)	k[a]	Detrended data τ_k (yr)
1715	157	17	430	79
1725	167	20	440	59
1735	176	21	450	40
1745	206	17	460	0
Douglas Fir AD 1145–1505				
1145	967	10	50	0
1155	907	15	60	43
1165	857	10	70	76
1175	881	14	80	35
1185	887	13	90	11
1195	857	14	100	24
1205	867	14	110	−3
1215	832	14	120	15
1225	795	10	130	35
1235	804	14	140	9
1245	803	14	150	−8
1255	811	14	160	−33
1265	755	15	170	6
1275	767	15	180	−23
1285	713	14	190	14
1295	661	15	200	49
1305	627	8	210	65
1315	625	10	220	50
1325	613	11	230	45
1335	560	10	240	81
1345	582	12	250	42
1355	617	12	260	−11
1365	604	11	270	−15
1375	653	11	280	−81
1385	633	11	290	−78
1395	575	14	300	−37
1405	565	13	310	−44
1415	520	14	320	−17
1425	500	13	330	−14
1435	468	14	340	1
1445	418	12	350	34
1455	390	10	360	45
1465	395	14	370	23
1475	390	14	380	11
1485	380	13	390	3
1495	353	10	400	13

Table 1 ^{14}C age of tree-ring dated wood of New Zealand Matai (*Prumnopitys taxifolia*) from Sparks et al. (1995: Table 2), Douglas Fir (*Pseudotsuga menziesii*) from Stuiver et al. (1998), and English Oak (*Quercus petroca*), and New Zealand Cedar (*Libocedrus bidwillii*) from McCormac et al. (1998) (*Continued*)

Calendar age (AD)	Conventional ^{14}C age (BP)	Standard error (yr)	k[a]	Detrended data τ_k (yr)
1505	349	8	410	0
Douglas Fir AD 1515–1945				
1515	349	5	40	0
1525	322	4	50	23
1535	301	3	60	41
1545	309	4	70	29
1555	319	5	80	15
1565	326	4	90	5
1575	329	5	100	−2
1585	333	4	110	−10
1595	340	4	120	−21
1605	365	4	130	−49
1615	351	4	140	−39
1625	333	4	150	−25
1635	308	4	160	−3
1645	268	4	170	33
1655	241	4	180	56
1665	209	4	190	85
1675	172	4	200	118
1685	139	3	210	147
1695	115	2	220	167
1705	105	3	230	174
1715	95	3	240	180
1725	114	3	250	157
1735	153	4	260	115
1745	163	4	270	101
1755	156	3	280	104
1765	169	4	290	88
1775	167	4	300	86
1785	216	5	310	33
1795	201	4	320	44
1805	159	4	330	83
1815	106	4	340	132
1825	99	3	350	135
1835	116	3	360	115
1845	115	4	370	112
1855	120	4	380	103
1865	117	4	390	103
1875	115	4	400	101
1885	100	3	410	112

Table 1 ^{14}C age of tree-ring dated wood of New Zealand Matai (*Prumnopitys taxifolia*) from Sparks et al. (1995: Table 2), Douglas Fir (*Pseudotsuga menziesii*) from Stuiver et al. (1998), and English Oak (*Quercus petroca*), and New Zealand Cedar (*Libocedrus bidwillii*) from McCormac et al. (1998) (*Continued*)

Calendar age (AD)	Conventional ^{14}C age (BP)	Standard error (yr)	k[a]	Detrended data τ_k (yr)
1895	76	3	420	132
1905	78	3	430	127
1915	108	3	440	93
1925	138	3	450	59
1935	156	4	460	38
1945	190	4	470	0
Oak AD 1725–1935				
1725	133	14	140	0
1735	176	14	150	−40
1745	205	14	160	−67
1755	208	18	170	−67
1765	195	13	180	−52
1775	184	13	190	−38
1785	217	13	200	−69
1795	210	14	210	−59
1805	122	14	220	32
1815	128	14	230	28
1825	107	14	240	52
1835	103	14	250	58
1845	137	14	260	27
1855	126	14	270	40
1865	126	11	280	43
1875	146	13	290	26
1885	129	14	300	45
1895	148	13	310	29
1905	109	13	320	70
1915	146	14	330	36
1925	145	14	340	39
1935	187	14	350	0
Cedar AD 1745–1935				
1725	148	14	140	0
1735	204	14	150	−55
1745	228	13	160	−79
1755	236	13	170	−86
1765	223	13	180	−73
1775	204	13	190	−53
1785	240	13	200	−89
1795	235	13	210	−83
1805	170	13	220	−17
1815	142	14	230	11

https://doi.org/10.1017/S0033822200031672 Published online by Cambridge University Press

Table 1 ^{14}C age of tree-ring dated wood of New Zealand Matai (*Prumnopitys taxifolia*) from Sparks et al. (1995: Table 2), Douglas Fir (*Pseudotsuga menziesii*) from Stuiver et al. (1998), and English Oak (*Quercus petroca*), and New Zealand Cedar (*Libocedrus bidwillii*) from McCormac et al. (1998) (*Continued*)

Calendar age (AD)	Conventional ^{14}C age (BP)	Standard error (yr)	k[a]	Detrended data τ_k (yr)
1825	146	14	240	8
1835	149	13	250	5
1845	156	14	260	−1
1855	167	14	270	−12
1865	161	11	280	−5
1875	151	10	290	6
1885	155	13	300	2
1895	129	12	310	29
1905	125	13	320	33
1915	118	14	330	41
1925	172	13	340	−13
1935	160	14	350	0

[a]k = the index number of the data point in the extended data set after zero padding.

https://doi.org/10.1017/S0033822200031672 Published online by Cambridge University Press

Table 6 Least-squares smoothed calibration curve at yearly intervals for New Zealand Matai (*Prumnopitys taxifolia*) (Sparks et al. 1995) between AD 1330 and AD 1750 corrected for a running mean over 10 tree rings. Mean standard error of the curve is 9 ± 3 yr.

Tree-ring date AD	^{14}C age (BP)	Tree-ring date AD	^{14}C age (BP)	Tree-ring date AD	^{14}C age (BP)	Tree-ring date AD	^{14}C age (BP)
1330	630	1363	649	1396	596	1429	485
1331	630	1364	649	1397	593	1430	482
1332	631	1365	649	1398	590	1431	479
1333	631	1366	649	1399	586	1432	477
1334	632	1367	649	1400	583	1433	474
1335	632	1368	649	1401	579	1434	472
1336	633	1369	649	1402	576	1435	470
1337	634	1370	648	1403	572	1436	468
1338	634	1371	647	1404	569	1437	466
1339	635	1372	646	1405	565	1438	463
1340	636	1373	645	1406	562	1439	462
1341	636	1374	644	1407	558	1440	460
1342	637	1375	643	1408	554	1441	458
1343	638	1376	642	1409	551	1442	456
1344	639	1377	641	1410	547	1443	454
1345	640	1378	639	1411	544	1444	453
1346	640	1379	638	1412	540	1445	451
1347	641	1380	636	1413	536	1446	450
1348	642	1381	635	1414	533	1447	449
1349	643	1382	633	1415	529	1448	447
1350	643	1383	631	1416	526	1449	446
1351	644	1384	629	1417	522	1450	445
1352	645	1385	626	1418	519	1451	444
1353	646	1386	624	1419	515	1452	443
1354	646	1387	622	1420	512	1453	442
1355	647	1388	619	1421	509	1454	441
1356	647	1389	617	1422	506	1455	440
1357	648	1390	614	1423	502	1456	439
1358	648	1391	611	1424	499	1457	438
1359	649	1392	608	1425	496	1458	437
1360	649	1393	605	1426	493	1459	436
1361	649	1394	602	1427	490	1460	435
1362	649	1395	599	1428	488	1461	435

https://doi.org/10.1017/S0033822200031672 Published online by Cambridge University Press

Table 6 Least-squares smoothed calibration curve at yearly intervals for New Zealand Matai (*Prumnopitys taxifolia*) (Sparks et al. 1995) between AD 1330 and AD 1750 corrected for a running mean over 10 tree rings. Mean standard error of the curve is 9 ± 3 yr. (*Continued*)

Tree-ring date AD	^{14}C age (BP)	Tree-ring date AD	^{14}C age (BP)	Tree-ring date AD	^{14}C age (BP)	Tree-ring date AD	^{14}C age (BP)
1462	434	1496	397	1530	332	1564	338
1463	433	1497	395	1531	331	1565	339
1464	433	1498	394	1532	330	1566	341
1465	432	1499	392	1533	329	1567	342
1466	431	1500	390	1534	328	1568	344
1467	430	1501	388	1535	327	1569	346
1468	430	1502	386	1536	326	1570	347
1469	429	1503	384	1537	325	1571	349
1470	428	1504	382	1538	324	1572	351
1471	427	1505	380	1539	324	1573	352
1472	427	1506	378	1540	323	1574	354
1473	426	1507	376	1541	323	1575	356
1474	425	1508	374	1542	322	1576	357
1475	424	1509	372	1543	322	1577	359
1476	423	1510	370	1544	322	1578	360
1477	422	1511	367	1545	322	1579	362
1478	422	1512	365	1546	322	1580	364
1479	421	1513	363	1547	322	1581	365
1480	420	1514	361	1548	322	1582	367
1481	418	1515	359	1549	323	1583	368
1482	417	1516	357	1550	323	1584	369
1483	416	1517	355	1551	324	1585	371
1484	415	1518	353	1552	324	1586	372
1485	414	1519	351	1553	325	1587	373
1486	413	1520	349	1554	326	1588	374
1487	411	1521	347	1555	327	1589	375
1488	410	1522	345	1556	328	1590	376
1489	408	1523	343	1557	329	1591	377
1490	407	1524	342	1558	330	1592	378
1491	405	1525	340	1559	331	1593	379
1492	404	1526	338	1560	332	1594	379
1493	402	1527	337	1561	333	1595	380
1494	401	1528	335	1562	335	1596	380
1495	399	1529	334	1563	336	1597	381

Table 6 Least-squares smoothed calibration curve at yearly intervals for New Zealand Matai (*Prumnopitys taxifolia*) (Sparks et al. 1995) between AD 1330 and AD 1750 corrected for a running mean over 10 tree rings. Mean standard error of the curve is 9 ± 3 yr. (*Continued*)

Tree-ring date AD	^{14}C age (BP)	Tree-ring date AD	^{14}C age (BP)	Tree-ring date AD	^{14}C age (BP)	Tree-ring date AD	^{14}C age (BP)
1598	381	1631	331	1665	221	1698	162
1599	381	1632	328	1666	218	1699	161
1600	381	1633	325	1667	215	1700	161
1601	381	1634	322	1668	212	1701	161
1602	381	1635	319	1669	209	1702	161
1603	380	1636	316	1670	206	1703	161
1604	380	1637	313	1671	204	1704	161
1605	379	1638	310	1672	201	1705	161
1606	379	1639	306	1673	199	1706	161
1607	378	1640	303	1674	196	1707	161
1608	377	1641	300	1675	194	1708	162
1609	376	1642	296	1676	191	1709	162
1610	375	1643	293	1677	189	1710	162
1611	374	1644	290	1678	187	1711	163
1612	373	1645	286	1679	185	1712	163
1613	371	1646	283	1680	183	1713	164
1614	370	1647	279	1681	181	1714	165
1615	368	1648	276	1682	179	1715	165
1616	367	1649	273	1683	177	1716	166
1617	365	1650	269	1684	176	1717	167
1618	363	1651	266	1685	174	1718	168
1619	361	1652	262	1686	173	1719	168
1620	359	1653	259	1687	171	1720	169
1621	357	1654	256	1688	170	1721	170
1622	355	1655	252	1689	169	1722	171
1623	352	1656	249	1690	168	1723	172
1624	350	1657	246	1691	167	1724	173
1625	348	1658	242	1692	166	1725	174
1626	345	1659	239	1693	165	1726	175
1627	342	1660	236	1694	164	1727	176
1628	340	1662	230	1695	163	1728	177
1629	337	1663	227	1696	163	1729	178
1630	334	1664	224	1697	162	1730	179

https://doi.org/10.1017/S0033822200031672 Published online by Cambridge University Press

Table 6 Least-squares smoothed calibration curve at yearly intervals for New Zealand Matai (*Prumnopitys taxifolia*) (Sparks et al. 1995) between AD 1330 and AD 1750 corrected for a running mean over 10 tree rings. Mean standard error of the curve is 9 ± 3 yr. (*Continued*)

Tree-ring date AD	^{14}C age (BP)	Tree-ring date AD	^{14}C age (BP)	Tree-ring date AD	^{14}C age (BP)	Tree-ring date AD	^{14}C age (BP)
1731	180	1739	186	1747	191		
1732	180	1740	187	1748	191		
1733	181	1741	188	1749	191		
1734	182	1742	188	1750	192		
1735	183	1743	189				
1736	184	1744	189				
1737	185	1745	190				
1738	185	1746	190				

https://doi.org/10.1017/S0033822200031672 Published online by Cambridge University Press

Table 7 Least-squares smoothed calibration curve at yearly intervals for North American Douglas Fir (*Pseudotsuga menziesii*) (Stuiver et al. 1998) between AD 1140 and AD 1510 corrected for a running mean over 10 tree rings. Mean standard error of the curve is 8 ± 3 yr.

Tree-ring date AD	^{14}C age (BP)	Tree-ring date AD	^{14}C age (BP)	Tree-ring date AD	^{14}C age (BP)	Tree-ring date AD	^{14}C age (BP)
1140	970	1178	871	1216	828	1254	804
1141	967	1179	871	1217	825	1255	803
1142	963	1180	871	1218	823	1256	802
1143	960	1181	872	1219	821	1257	800
1144	956	1182	872	1220	819	1258	799
1145	952	1183	872	1221	817	1259	797
1146	949	1184	873	1222	815	1260	795
1147	945	1185	873	1223	813	1261	793
1148	941	1186	873	1224	811	1262	790
1149	937	1187	874	1225	810	1263	788
1150	933	1188	874	1226	809	1264	785
1151	929	1189	874	1227	808	1265	782
1152	925	1190	874	1228	807	1266	779
1153	921	1191	874	1229	806	1267	776
1154	917	1192	873	1230	805	1268	773
1155	913	1193	873	1231	805	1269	769
1156	910	1194	872	1232	804	1270	766
1157	906	1195	872	1233	804	1271	762
1158	903	1196	871	1234	804	1272	758
1159	899	1197	870	1235	804	1273	754
1160	896	1198	868	1236	804	1274	750
1161	893	1199	867	1237	804	1275	746
1162	890	1200	865	1238	804	1276	742
1163	888	1201	864	1239	805	1277	738
1164	885	1202	862	1240	805	1278	734
1165	883	1203	860	1241	805	1279	730
1166	881	1204	858	1242	805	1280	725
1167	879	1205	856	1243	806	1281	721
1168	877	1206	853	1244	806	1282	717
1169	876	1207	851	1245	806	1283	713
1170	875	1208	848	1246	806	1284	709
1171	874	1209	846	1247	807	1285	705
1172	873	1210	843	1248	807	1286	701
1173	872	1211	841	1249	806	1287	697
1174	872	1212	838	1250	806	1288	694
1175	871	1213	835	1251	806	1289	690
1176	871	1214	833	1252	805	1290	686
1177	871	1215	830	1253	805	1291	683

Table 7 Least-squares smoothed calibration curve at yearly intervals for North American Douglas Fir (*Pseudotsuga menziesii*) (Stuiver et al. 1998) between AD 1140 and AD 1510 corrected for a running mean over 10 tree rings. Mean standard error of the curve is 8 ± 3 yr. (*Continued*)

Tree-ring date AD	^{14}C age (BP)	Tree-ring date AD	^{14}C age (BP)	Tree-ring date AD	^{14}C age (BP)	Tree-ring date AD	^{14}C age (BP)
1292	680	1330	630	1368	649	1406	553
1293	676	1331	630	1369	649	1407	550
1294	673	1332	631	1370	648	1408	547
1295	670	1333	631	1371	647	1409	543
1296	667	1334	632	1372	646	1410	540
1297	664	1335	632	1373	645	1411	537
1298	661	1336	633	1374	644	1412	534
1299	658	1337	634	1375	643	1413	532
1300	656	1338	634	1376	642	1414	529
1301	653	1339	635	1377	641	1415	526
1302	650	1340	636	1378	639	1416	523
1303	648	1341	636	1379	638	1417	520
1304	645	1342	637	1380	636	1418	517
1305	643	1343	638	1381	635	1419	514
1306	640	1344	639	1382	633	1420	511
1307	638	1345	640	1383	631	1421	508
1308	636	1346	640	1384	629	1422	504
1309	633	1347	641	1385	626	1423	501
1310	631	1348	642	1386	624	1424	498
1311	629	1349	643	1387	622	1425	495
1312	626	1350	643	1388	619	1426	491
1313	624	1351	644	1389	617	1427	488
1314	622	1352	645	1390	614	1428	484
1315	619	1353	646	1391	611	1429	481
1316	617	1354	598	1392	608	1430	477
1317	615	1355	601	1393	605	1431	474
1318	612	1356	603	1394	602	1432	470
1319	610	1357	606	1395	599	1433	466
1320	608	1358	609	1396	596	1434	462
1321	605	1359	611	1397	593	1435	459
1322	603	1360	614	1398	590	1436	455
1323	601	1361	616	1399	586	1437	451
1324	599	1362	619	1400	583	1438	448
1325	597	1363	621	1401	579	1439	444
1326	595	1364	623	1402	576	1440	440
1327	592	1365	625	1403	572	1441	437
1328	591	1366	627	1404	569	1442	433
1329	589	1367	629	1405	565	1443	430

Table 7 Least-squares smoothed calibration curve at yearly intervals for North American Douglas Fir (*Pseudotsuga menziesii*) (Stuiver et al. 1998) between AD 1140 and AD 1510 corrected for a running mean over 10 tree rings. Mean standard error of the curve is 8 ± 3 yr. (*Continued*)

Tree-ring date AD	^{14}C age (BP)	Tree-ring date AD	^{14}C age (BP)	Tree-ring date AD	^{14}C age (BP)	Tree-ring date AD	^{14}C age (BP)
1444	426	1461	390	1478	383	1495	363
1445	423	1462	389	1479	382	1496	361
1446	420	1463	388	1480	382	1497	360
1447	417	1464	388	1481	418	1498	358
1448	414	1465	387	1482	417	1499	356
1449	411	1466	387	1483	416	1500	354
1450	409	1467	386	1484	378	1501	352
1451	406	1468	386	1485	377	1502	350
1452	404	1469	386	1486	376	1503	349
1453	402	1470	385	1487	375	1504	347
1454	400	1471	385	1488	374	1505	345
1455	398	1472	385	1489	372	1506	343
1456	396	1473	385	1490	371	1507	342
1457	395	1474	384	1491	370	1508	340
1458	393	1475	384	1492	368	1509	338
1459	392	1476	384	1493	366	1510	337
1460	391	1477	383	1494	365		

https://doi.org/10.1017/S0033822200031672 Published online by Cambridge University Press

Table 8 Least-squares smoothed calibration curve at yearly intervals for North American Douglas Fir (*Pseudotsuga menziesii*) (Stuiver et al. 1998) between AD 1510 and AD 1950 corrected for a running mean over 10 tree rings. Mean standard error of the curve is 3 ± 1 yr.

Tree-ring date AD	^{14}C age (yr BP)	Tree-ring date AD	^{14}C age (yr BP)	Tree-ring date AD	^{14}C age (yr BP)	Tree-ring date AD	^{14}C age (yr BP)
1510	353	1553	318	1596	348	1639	290
1511	352	1554	319	1597	349	1640	287
1512	351	1555	321	1598	351	1641	284
1513	350	1556	322	1599	353	1642	281
1514	348	1557	323	1600	354	1643	278
1515	347	1558	325	1601	355	1644	275
1516	345	1559	326	1602	356	1645	272
1517	343	1560	326	1603	357	1646	269
1518	341	1561	327	1604	358	1647	266
1519	338	1562	328	1605	359	1648	262
1520	336	1563	328	1606	359	1649	259
1521	333	1564	328	1607	360	1650	256
1522	331	1565	328	1608	360	1651	253
1523	328	1566	328	1609	360	1652	250
1524	325	1567	328	1610	360	1653	247
1525	323	1568	328	1611	359	1654	244
1526	320	1569	328	1612	359	1655	241
1527	317	1570	328	1613	358	1656	238
1528	315	1571	327	1614	357	1657	235
1529	312	1572	327	1615	356	1658	231
1530	310	1573	327	1616	354	1659	228
1531	308	1574	327	1617	353	1660	225
1532	306	1575	326	1618	351	1661	221
1533	305	1576	326	1619	349	1662	218
1534	303	1577	326	1620	347	1663	215
1535	302	1578	326	1621	345	1664	211
1536	301	1579	327	1622	342	1665	208
1537	301	1580	327	1623	340	1666	204
1538	300	1581	328	1624	337	1667	200
1539	300	1582	328	1625	334	1668	197
1540	300	1583	329	1626	331	1669	193
1541	301	1584	330	1627	329	1670	190
1542	302	1585	331	1628	326	1671	186
1543	302	1586	332	1629	322	1672	182
1544	304	1587	333	1630	319	1673	179
1545	305	1588	335	1631	316	1674	175
1546	306	1589	336	1632	313	1675	172
1547	308	1590	338	1633	310	1676	168
1548	309	1591	339	1634	307	1677	165
1549	311	1592	341	1635	303	1678	161
1550	313	1593	343	1636	300	1679	158
1551	314	1594	344	1637	297	1680	155
1552	316	1595	346	1638	294	1681	152

https://doi.org/10.1017/S0033822200031672 Published online by Cambridge University Press

Table 8 Least-squares smoothed calibration curve at yearly intervals for North American Douglas Fir (*Pseudotsuga menziesii*) (Stuiver et al. 1998) between AD 1510 and AD 1950 corrected for a running mean over 10 tree rings. Mean standard error of the curve is 3 ± 1 yr. (*Continued*)

Tree-ring date AD	^{14}C age (yr BP)	Tree-ring date AD	^{14}C age (yr BP)	Tree-ring date AD	^{14}C age (yr BP)	Tree-ring date AD	^{14}C age (yr BP)
1682	149	1725	116	1768	160	1811	124
1683	146	1726	119	1769	162	1812	119
1684	143	1727	122	1770	164	1813	115
1685	140	1728	125	1771	166	1814	111
1686	137	1729	128	1772	169	1815	108
1687	134	1730	131	1773	172	1816	105
1688	132	1731	135	1774	175	1817	102
1689	129	1732	138	1775	178	1818	101
1690	127	1733	141	1776	182	1819	99
1691	125	1734	144	1777	185	1820	98
1692	122	1735	147	1778	189	1821	97
1693	120	1736	150	1779	192	1822	97
1694	118	1737	153	1780	196	1823	97
1695	116	1738	155	1781	199	1824	98
1696	114	1739	157	1782	202	1825	98
1697	112	1740	160	1783	205	1827	101
1698	110	1741	161	1784	208	1828	102
1699	109	1742	163	1785	210	1829	103
1700	107	1743	164	1786	212	1830	105
1701	106	1744	165	1787	213	1831	107
1702	104	1745	166	1788	214	1832	108
1703	103	1746	167	1789	214	1833	110
1704	102	1747	167	1790	214	1834	111
1705	100	1748	167	1791	214	1835	113
1706	99	1749	167	1792	213	1836	114
1707	99	1750	166	1793	211	1837	115
1708	98	1751	165	1794	208	1838	116
1709	97	1752	165	1795	206	1839	117
1710	97	1753	164	1796	202	1840	118
1711	97	1754	163	1797	199	1841	119
1712	97	1755	162	1798	194	1842	119
1713	97	1756	160	1799	190	1843	119
1714	97	1757	159	1800	185	1844	119
1715	98	1758	158	1801	179	1845	119
1716	99	1759	158	1802	174	1846	119
1717	100	1760	157	1803	168	1847	119
1718	101	1761	156	1804	162	1848	119
1719	103	1762	156	1805	156	1849	118
1720	104	1763	156	1806	151	1850	118
1721	106	1764	156	1807	145	1851	118
1722	108	1765	157	1808	139	1852	117
1723	111	1766	157	1809	134	1853	117
1724	113	1767	159	1810	129	1854	117

https://doi.org/10.1017/S0033822200031672 Published online by Cambridge University Press

Table 8 Least-squares smoothed calibration curve at yearly intervals for North American Douglas Fir (*Pseudotsuga menziesii*) (Stuiver et al. 1998) between AD 1510 and AD 1950 corrected for a running mean over 10 tree rings. Mean standard error of the curve is 3 ± 1 yr. (*Continued*)

Tree-ring date AD	^{14}C age (yr BP)	Tree-ring date AD	^{14}C age (yr BP)	Tree-ring date AD	^{14}C age (yr BP)	Tree-ring date AD	^{14}C age (yr BP)
1855	117	1879	110	1903	77	1927	142
1856	116	1880	109	1904	78	1928	145
1857	116	1881	107	1905	80	1929	148
1858	117	1882	104	1906	81	1930	151
1859	117	1883	102	1907	83	1931	153
1860	117	1884	100	1908	86	1932	156
1861	117	1885	97	1909	88	1933	159
1862	117	1886	95	1910	91	1934	161
1863	118	1887	92	1911	93	1935	164
1864	118	1888	90	1912	96	1936	166
1865	118	1889	87	1913	99	1937	168
1866	119	1890	85	1914	102	1938	171
1867	119	1891	83	1915	105	1939	173
1868	119	1892	81	1916	108	1940	175
1869	119	1893	79	1917	112	1941	177
1870	119	1894	78	1918	115	1942	178
1871	119	1895	77	1919	118	1943	180
1872	119	1896	76	1920	121	1944	182
1873	118	1897	75	1921	124	1945	183
1874	117	1898	74	1922	127	1946	184
1875	116	1899	74	1923	130	1947	186
1876	115	1900	74	1924	133	1948	187
1877	114	1901	75	1925	136	1949	187
1878	112	1902	76	1926	139	1950	188

Table 9 Least-squares smoothed calibration curve at yearly intervals for English Oak (*Quercus petroca*) (McCormac et al. 1998) between AD 1720 and AD 1940 corrected for a running mean over 10 tree rings. Mean standard error of the curve is 8 ± 4 yr.

Tree-ring date AD	^{14}C age (BP)	Tree-ring date AD	^{14}C age (BP)	Tree-ring date AD	^{14}C age (BP)	Tree-ring date AD	^{14}C age (BP)
1720	131	1762	201	1804	153	1846	128
1721	132	1763	200	1805	149	1847	128
1722	134	1764	200	1806	145	1848	127
1723	136	1765	199	1807	141	1849	127
1724	138	1766	199	1808	137	1850	127
1725	140	1767	199	1809	133	1851	126
1726	143	1768	199	1810	130	1852	126
1727	146	1769	199	1811	126	1853	126
1728	148	1770	199	1812	123	1854	125
1729	151	1771	199	1813	121	1855	125
1730	154	1772	199	1814	118	1856	125
1731	158	1773	199	1815	116	1857	124
1732	161	1774	200	1816	114	1858	124
1733	164	1775	200	1817	112	1859	124
1734	168	1776	201	1818	111	1860	124
1735	171	1777	201	1819	110	1861	124
1736	174	1778	202	1820	109	1862	125
1737	178	1779	202	1821	109	1863	125
1738	181	1780	203	1822	108	1864	126
1739	184	1781	203	1823	108	1865	126
1740	187	1782	203	1824	109	1866	127
1741	189	1783	203	1825	109	1867	128
1742	192	1784	203	1826	110	1868	129
1743	194	1785	203	1827	111	1869	130
1744	196	1786	203	1828	112	1870	131
1745	198	1787	202	1829	113	1871	132
1746	200	1788	201	1830	114	1872	133
1747	201	1789	200	1831	116	1873	134
1748	202	1790	198	1832	117	1874	135
1749	203	1791	196	1833	118	1875	136
1750	204	1792	194	1834	120	1876	137
1751	205	1793	192	1835	121	1877	138
1752	205	1794	190	1836	122	1878	139
1753	205	1795	187	1837	123	1879	140
1754	205	1796	184	1838	124	1880	141
1755	205	1797	180	1839	125	1881	141
1756	204	1798	177	1840	126	1882	142
1757	204	1799	173	1841	126	1883	142
1758	203	1800	169	1842	127	1884	142
1759	203	1801	165	1843	127	1885	142
1760	202	1802	161	1844	128	1886	142
1761	201	1803	157	1845	128	1887	142

Table 9 Least-squares smoothed calibration curve at yearly intervals for English Oak (*Quercus petroca*) (McCormac et al. 1998) between AD 1720 and AD 1940 corrected for a running mean over 10 tree rings. Mean standard error of the curve is 8 ± 4 yr. (*Continued*)

Tree-ring date AD	^{14}C age (BP)	Tree-ring date AD	^{14}C age (BP)	Tree-ring date AD	^{14}C age (BP)	Tree-ring date AD	^{14}C age (BP)
1888	141	1904	128	1920	144	1936	179
1889	141	1905	127	1921	146	1937	181
1890	140	1906	127	1922	149	1938	182
1891	139	1907	127	1923	151	1939	184
1892	138	1908	127	1924	154	1940	185
1893	137	1909	128	1925	156		
1894	136	1910	128	1926	159		
1895	135	1911	129	1927	161		
1896	134	1912	130	1928	163		
1897	133	1913	131	1929	166		
1898	132	1914	133	1930	168		
1899	131	1915	134	1931	170		
1900	130	1916	136	1932	172		
1901	129	1917	138	1933	174		
1902	129	1918	140	1934	176		
1903	128	1919	142	1935	178		

Table 10 Least-squares smoothed calibration curve at yearly intervals for New Zealand Cedar (*Libocedrus bidwillii*) (McCormac et al. 1998) between AD 1720 and AD 1940 corrected for a running mean over 10 tree rings. Mean standard error of the curve is 8 ± 4 yr.

Tree-ring date AD	^{14}C age (BP)	Tree-ring date AD	^{14}C age (BP)	Tree-ring date AD	^{14}C age (BP)	Tree-ring date AD	^{14}C age (BP)
1720	148	1762	223	1804	185	1846	163
1721	149	1763	222	1805	181	1847	162
1722	151	1764	221	1806	176	1848	162
1723	153	1765	220	1807	172	1849	161
1724	156	1766	219	1808	168	1850	160
1725	158	1767	218	1809	164	1851	160
1726	161	1768	218	1810	160	1852	159
1727	164	1769	218	1811	157	1853	158
1728	168	1770	218	1812	153	1854	157
1729	171	1771	218	1813	150	1855	156
1730	175	1772	218	1814	148	1856	156
1731	179	1773	218	1815	146	1857	155
1732	183	1774	219	1816	144	1858	155
1733	187	1775	220	1817	142	1859	154
1734	191	1776	221	1818	141	1860	154
1735	195	1777	222	1819	140	1861	154
1736	199	1778	223	1820	139	1862	154
1737	203	1779	224	1821	139	1863	154
1738	207	1780	225	1822	139	1864	154
1739	210	1781	226	1823	140	1865	154
1740	214	1782	227	1824	141	1866	154
1741	217	1783	228	1825	142	1867	155
1742	220	1784	229	1826	143	1868	155
1743	223	1785	229	1827	144	1869	156
1744	225	1786	230	1828	146	1870	156
1745	227	1787	230	1829	147	1871	157
1746	229	1788	229	1830	149	1872	157
1747	231	1789	229	1831	150	1873	157
1748	232	1790	228	1832	152	1874	158
1749	233	1791	227	1833	154	1875	158
1750	233	1792	225	1834	155	1876	158
1751	233	1793	224	1835	157	1877	158
1752	233	1794	221	1836	158	1878	158
1753	233	1795	219	1837	160	1879	158
1754	232	1796	216	1838	161	1880	157
1755	232	1797	213	1839	162	1881	157
1756	231	1798	210	1840	162	1882	156
1757	230	1799	206	1841	163	1883	155
1758	228	1800	202	1842	163	1884	153
1759	227	1801	198	1843	163	1885	152
1760	226	1802	194	1844	163	1886	151
1761	225	1803	189	1845	163	1887	149

https://doi.org/10.1017/S0033822200031672 Published online by Cambridge University Press

Table 10 Least-squares smoothed calibration curve at yearly intervals for New Zealand Cedar (*Libocedrus bidwillii*) (McCormac et al. 1998) between AD 1720 and AD 1940 corrected for a running mean over 10 tree rings. Mean standard error of the curve is 8 ± 4 yr. (*Continued*)

Tree-ring date AD	^{14}C age (BP)	Tree-ring date AD	^{14}C age (BP)	Tree-ring date AD	^{14}C age (BP)	Tree-ring date AD	^{14}C age (BP)
1888	147	1907	122	1926	156		
1889	145	1908	123	1927	158		
1890	143	1909	124	1928	159		
1891	141	1910	125	1929	160		
1892	139	1911	126	1930	161		
1893	137	1912	128	1931	162		
1894	135	1913	128	1932	163		
1895	133	1914	131	1933	164		
1896	131	1915	133	1934	164		
1897	129	1916	135	1935	164		
1898	128	1917	137	1936	165		
1899	126	1918	139	1937	165		
1900	125	1919	142	1938	165		
1901	124	1920	144	1939	164		
1902	123	1921	146	1940	164		
1903	122	1922	148				
1904	122	1923	150				
1905	122	1924	152				
1906	122	1925	154				